Supporting Information

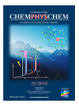

Ultrafast Charge Dynamics in Mixed Cation – Mixed Halide Perovskite Thin Films

Iulia Minda,* Jonas Horn, Essraa Ahmed, Derck Schlettwein, and Heinrich Schwoerer

Supporting Information

A. Variation of Perovskite composition

The collection of thin films which were measured to compare the different chemical compositions included four samples for each material, two of which were encapsulated with PMMA and two with glass and epoxy. These include: the primary material under investigation $FA_{0.85}MA_{0.15}PbI_{2.55}Br_{0.45}$, $FA_{0.85}MA_{0.15}PbI_3$, $FA_{0.5}MA_{0.5}PbI_3$, $FAPbI_3$ and $FA_{0.5}MA_{0.5}PbI_{1.5}Br_{1.5}$. Five representative transient absorption spectra, acquired in the visible spectral region, are presented in Figure 1, together with the associated perovskite material chemical compositions and vertical lineouts of the change in optical density as a function of wavelength ($\Delta OD(\lambda)$).

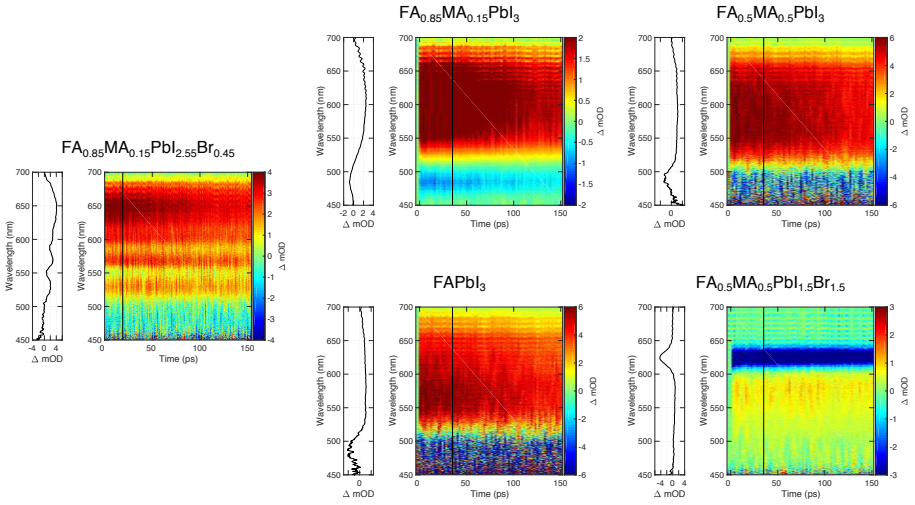

Figure 1: Five representative transient absorption spectra, acquired in the visible spectral region, are presented together with the associated perovskite material chemical compositions and vertical lineouts of the change in optical density as a function of wavelength. The leftmost transient corresponds to the primary material under investigation $FA_{0.85}MA_{0.15}PbI_{2.55}Br_{0.45}$, where a clear three-band ESA1 signal can be observed. A broadband ESA1 signal with no spectral structure is observed for the remaining transients: $FA_{0.85}MA_{0.15}PbI_3$ (top left), $FA_{0.5}MA_{0.5}PbI_3$ (top right), $FAPbI_3$ (bottom left) and $FA_{0.5}MA_{0.5}PbI_{1.5}Br_{1.5}$ (bottom right).

All of the transient absorption spectra presented in Figure 1, except that of $FA_{0.85}MA_{0.15}PbI_{2.55}Br_{0.45}$, contain a broad positive absorption signal corresponding to ESA1 without any distinct multi-band feature. We therefore assign the three-band spectral structure of the ESA1 signal as unique to $FA_{0.85}MA_{0.15}PbI_{2.55}Br_{0.45}$. Additionally, the optical bandgap ground state bleaching signals are not dominant due to the low fluence pump pulses employed for these

measurements.

A possible explanation for this is that the mixture of methylammonium cations with larger formamidinium molecules introduces a distortion of the perovskite crystal structure. Furthermore, it increases the possible spatial orientation permutations of the organic ions within the lead halide framework. This leads to an increased loss of degeneracy in the multiple conduction and valence bands of mixed methylammonium - formamidinium perovskite materials with respect to their single organic cation counterparts.

Furthermore, as expected, the substitution of I^- with Br^-, causes a shift in the bandgap (and therefore the GSB1 signal) towards higher energies. This can directly be observed in the TAS measurements of $FA_{0.85}MA_{0.15}PbI_{2.55}Br_{0.45}$ (leftmost spectrum) and $FA_{0.5}MA_{0.5}PbI_{1.5}Br_{1.5}$ (bottom right spectrum). Interestingly, the higher energy bleaching signal (GSB2) also appears to have shifted to higher energies for the bromine containing perovskites and is centred about $\lambda = 460$ nm instead of $\lambda = 480$ nm. This shift indicates that the energies of the states which govern the electronic transition associated with GSB2, are determined by the orbitals of the halogen anion. Therefore the source of the GSB2, is strongly dependent on the halogen content of the perovskite material.

B. Variation of pump photon energy

The transient absorption data presented in this manuscript corresponded to the non-resonant photoexcitation of the perovskite thin films with a femtosecond laser pulse of 3.2 eV photon energy ($\lambda = 388$ nm), way above the bandgap. In addition, we also carried out measurements employing 2.6 eV and 1.6 eV photon energies ($\lambda = 480$ nm and $\lambda = 775$ nm). These resonant photoexcitation energies correspond directly to the two photoinduced ground state bleaching signals observed: GSB1 (bandgap electronic transition at the R-point), and GSB2 (electronic transition near to the M-point).

Although a series of TAS measurements were obtained and analysed, rather than presenting a collection of transient absorption spectra, the results are summarised in a sketch to aid with the explanation. Figure 2 is a drawing of the conduction and valence bands in $FA_{0.85}MA_{0.15}PbI_{2.55}Br_{0.45}$ which take part in the initial photophysics occurring upon optical pumping with an ultrashort laser pulse. In addition to the energy levels which are drawn as a function of the k vector, the observed spectroscopic signals are also shown. In addition, the three different photoexcitation energies are indicated with their associated central wavelengths. Observations pertaining to the four visible and near infrared spectroscopic signatures: GSB1, GSB2, ESA1 and ESA2, are also shown in the figure. The following discussion aims to support our assignment of spectral signatures and thus the charge dynamics model presented, by explaining these observations in more detail.

The spectral behaviour of the transient absorption spectra acquired with lower photon energy excitation (1.6 eV and 2.6 eV) was found to be very similar to that of photoexcitation with 3.2 eV photon energy. The spectral features assigned to **GSB1 and ESA1**, probing the electron population at the CB minimum, are present in the same spectral regions for all three sets of measurements.

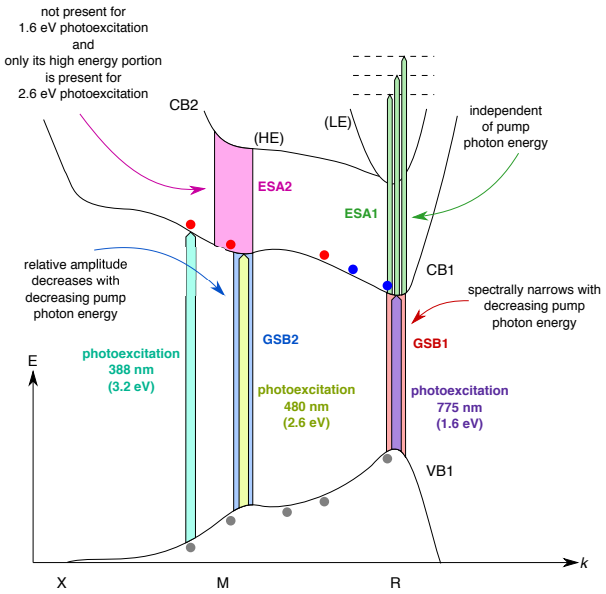

Figure 2: A simplified energy level diagram of the two lowest conduction bands (CB1 and CB2) and highest valence band (VB2) in $FA_{0.85}MA_{0.15}PbI_{2.55}Br_{0.45}$ drawn as a function of the k vector. Both the heavy (HE) and light (LE) electron portions of CB2 are depicted. The three photoexcitation energies employed in the TAS measurements are shown: 3.2 eV (turquoise), 2.6 eV (mustard) and 1.6 eV (purple). The effects of pumping with lower photon energies are summarised in the sketch for the spectroscopic signatures corresponding to: GSB1 (red), GSB2 (blue), ESA1 (green), ESA2 (pink).

Moreover the three-band spectral shape of ESA1 is observed irrespective of the pump energy with matching central wavelengths. The spectral broadness of the GSB1 signal is narrowed upon pumping with lower pump energies. This is due to a decrease in the hot charge carrier density and thus confirms our assignment of the charge carrier cooling dynamic.

As reported in literature, the **GSB2** signal is also present with lower photon energy excitation. Its relative amplitude with respect to the GSB1 signal is considerably smaller than in the case with 3.2 eV excitation (where it was already very weak) and diminishes with decreasing pump energy. This indicates a strongly reduced electron and hole population away from the R-point, upon lower energy photoexcitation.

We did not detect hot electrons in the conduction band away from the R-point upon pumping with 1.6 eV photon energy (corresponding to the optical bandgap of the perovskite material) as indicated by the lack of **ESA2** signal in the near infrared spectral region. Additionally, only the high energy portion of the signal is detected with 2.6 eV excitation, thereby directly confirming that the ESA2 signal corresponds to the absorption of the hot electron population in

the conduction band near to the M-point, which is only generated with sufficient pump laser pulse photon energies.

Finally, as an additional note, we observed that the temporal behaviour of the GSB1 and GSB2 signals is different upon bandgap photoexcitation (1.6 eV). This indicates that GSB1 and GSB2 correspond to the absorption of two different electron and hole populations, and fits with their assignment to the R- and M-points respectively.